

## QUANTIFICATION OF ALLOPHANE FROM ECUADOR

STEPHAN KAUFHOLD<sup>1</sup>, KRISTIAN UFER<sup>2</sup>, ANNETTE KAUFHOLD<sup>3</sup>, JOSEPH W. STUCKI<sup>4</sup>,  
ALEXANDRE S. ANASTÁCIO<sup>4</sup>, REINHOLD JAHN<sup>3</sup>, AND REINER DOHRMANN<sup>1,5</sup>

<sup>1</sup> BGR, Bundesanstalt für Geowissenschaften und Rohstoffe, Stilleweg 2, D-30655 Hannover, Germany

<sup>2</sup> TU Bergakademie Freiberg, Institute of Mineralogy, 09596 Freiberg, Germany

<sup>3</sup> Martin-Luther-University Halle-Wittenberg, Institute for Soil Sciences and Plant Nutrition, Weidenplan 14, D-06108 Halle, Germany

<sup>4</sup> Department of Natural Resources and Environmental Sciences, University of Illinois, Urbana, Illinois, USA

<sup>5</sup> LBEG, Landesamt für Bergbau, Energie und Geologie, Stilleweg 2, D-30655 Hannover, Germany

**Abstract**—Allophane is a very fine-grained clay mineral which is especially common in Andosols. Its importance in soils derives from its large reactive surface area. Owing to its short-range order, allophane cannot be quantified by powder X-ray diffraction (XRD) directly. It is commonly dissolved from the soil by applying extraction methods. In the present study the standard extraction method (oxalate) was judged to be unsuitable for the quantification of allophane in a soil/clay deposit from Ecuador, probably because of the large allophane content (>60 wt.%). This standard extraction method systematically underestimated the allophane content but the weakness was less pronounced in samples with small allophane contents. In the case of allophane-rich materials, the Rietveld XRD technique, using an internal standard to determine the sum of X-ray amorphous phases, is recommended if appropriate structural models are available for the other phases present in the sample. The allophane (+imogolite) content is measured by subtracting the amount of oxalate-soluble phases (*e.g.* ferrihydrite). No correction would be required if oxalate-soluble Fe were incorporated in the allophane structure. The present study, however, provides no evidence for this hypothesis. Mössbauer and scanning electron microscopy investigations indicate that goethite and poorly ordered hematite are the dominant Fe minerals and occur as very fine grains (or coatings) being dispersed in the cloud-like allophane aggregates.

Allophane is known to adsorb appreciable amounts of water, depending on ambient conditions. The mass fraction of the sample attributed to this mineral thus changes accordingly; the choice of a reference hydration state is, therefore, a fundamental factor in the quantification of allophane in a sample. Results from the present study revealed that (1) drying at 105°C produced a suitable reference state, and (2) water adsorption has no effect on quantification by XRD analysis.

**Key Words**—Allophane, Chemical Extraction Methods, Differential Thermal Analysis, Ecuador, Mössbauer Spectroscopy, Quantification, X-ray Diffraction.

### INTRODUCTION

Allophane is an X-ray-amorphous hydrous aluminum silicate clay mineral and consists of hollow spheres with a diameter ranging from 3 to 5 nm (*e.g.* Parfitt, 1990, 2009). Its idealized chemical formula is  $\text{Al}_2\text{O}_3 \cdot (\text{SiO}_2)_{1.3-2.5} - 3(\text{H}_2\text{O})$  and hence is characterized by its Al/Si ratio. Allophane is one of the first mineral alteration products from volcanic ash and, hence, can be found in weathered pumices and soils formed from young volcanic ash (Andosols). Due to its large reactive surface area, allophane can dominate the properties of soils (*e.g.* phosphate- and water-retention capacity) even if present in only minor amounts. Allophane is frequently accompanied by imogolite, its fibrous analogue.

Almost all scientific disciplines dealing with clays or soils need accurate values for mineral contents (*e.g.* for

modeling pollutant migration and retention). Many methods exist to quantify mineralogical composition and can be classified either as ‘chemical’ or ‘physical.’ ‘Chemical’ methods are based on selective extraction or adsorption of specific molecules (*e.g.* water). ‘Physical’ methods include XRD, infrared (IR) spectroscopy, and differential thermal analysis (DTA), among others. In their review articles, Dahlgren (1994) and Harsh (2000) presented strategies for the analysis of allophanes in soils. However, each of the available methods has its strengths and weaknesses. As an example, extraction methods may suffer from selectivity and/or incomplete dissolution. Several studies proved that the well established ammonium-oxalate extraction technique either fails to dissolve allophane entirely or also partially dissolves halloysite and/or gibbsite (*e.g.* Buurmann *et al.*, 2001; Dohrmann *et al.*, 2002). On the other hand, XRD-based methods – particularly the Rietveld technique – for clay-mineral quantification have been improved significantly in recent years (Ufer *et al.*, 2004, 2008) so that the characterization of minerals with short-range order, such as allophane, may be possible.

\* E-mail address of corresponding author:

s.kaufhold@bgr.de

DOI: 10.1346/CCMN.2010.0580509

Poor allophane diffraction intensities are caused by short-range order rather than by a specific type of disorder, as previously thought, so the use of improved XRD methods may provide an accurate structural model, describing the allophane XRD intensities, which heretofore has been lacking. Dohrmann *et al.* (2002) suggested that the addition of an internal standard would improve the chances for successful quantification of the amount of non-crystalline phases by the XRD methods.

The objective of this study was to apply and assess the improved XRD methods for quantifying allophane in soils using samples from the allophane vertical sequence investigated previously by Kaufhold *et al.* (2009). The ammonium oxalate method described by Schwertmann (1964) and Blakemore *et al.* (1981) is the most commonly used method to quantify allophane, so it was used as the reference method in this study.

## MATERIALS AND METHODS

Sixteen samples from an allophane-rich layer in Ecuador (Kaufhold, 2007) were selected. The samples and locations were described in detail by Kaufhold *et al.* (2009). Standard extraction methods (pyrophosphate, dithionite, ammonium oxalate) were performed according to Blakemore *et al.* (1981, 1987) and the amount of allophane was calculated according to Parfitt and Wilson (1985). In addition, one allophane (PM4-6) sample was selected to study the variation of the solid/liquid ratio during extraction in order to verify that all allophane actually dissolves at sufficiently low solid/liquid ratios.

Thermoanalytical investigations were performed using a Netzsch 409 PC thermobalance equipped with a DSC/TG sample holder linked to a Pfeiffer Thermstar quadrupole mass spectrometer (MS). 100 mg of powdered material, previously equilibrated at 53% relative humidity (r.h.), was heated from 25 to 1000°C at a heating rate of 10 K/min.

The chemical composition of powdered samples was determined using a PANalytical Axios and a PW2400 spectrometer. Samples were prepared by mixing with a flux material and melting into glass beads. The beads were analyzed by wavelength-dispersive X-ray fluorescence spectrometry (WD-XRF). To determine loss on ignition (LOI), 1000 mg of sample material was heated to 1030°C for 10 min and then weighed after cooling in a desiccator.

### *X-ray diffraction (XRD)*

Prior to XRD measurements, samples were ground in a McCrone mill using agate grinding elements, and an internal standard (10.0 wt.% zincite for samples 1 to 9 and 10.0 wt.% corundum for samples 10 to 16) was added for indirect quantification of allophane content. Both internal standards were compared and both are applicable (this does not affect the results).

All samples were measured in Bragg-Brentano geometry. For all specimen preparation, the top-loading technique was used. Samples 1 to 9 were measured on a 3003TT (Seifert) diffractometer (CuK $\alpha$  radiation generated at 40 kV and 40 mA) equipped with an automatic divergence slit irradiating 15 mm sample length, a 0.5 mm detector slit, a diffracted-beam graphite monochromator, and a proportional counter. The XRD patterns of samples 10 to 16 were recorded using a Philips X'Pert PW3710  $\theta$ - $2\theta$  diffractometer (CuK $\alpha$  radiation generated at 40 kV and 40 mA) equipped with a 1° divergence slit, a 0.2 mm detector slit, a diffracted-beam graphite monochromator, and a scintillation detector. The samples were measured from 2° to 80° $2\theta$  with a step size of 0.02° $2\theta$  and a measuring time of 3 s per step (Philips) or 0.03° $2\theta$  and 10 s (Seifert). For the XRD measurement under different humidity conditions, the Seifert diffractometer was equipped with a controlled atmosphere chamber ('TC basic', MRI, Karlsruhe, Germany) into which air at different r.h. was introduced. The different air humidity loads were generated outside the chamber by a r.h. calibrator ('rH-Cal', EdgeTech Moisture and Humidity, Marlborough, Massachusetts, USA) and supplied to the sample chamber *via* temperature-isolated hoses. The humidity in the chamber was checked at its outlet port using a hand-held r.h. analyzer. The r.h.-dependent XRD measurements were then obtained at room temperature from 2° to 80° $2\theta$  with a step size of 0.03° $2\theta$  and a measuring time of 3 s per step.

### *Rietveld refinements*

The XRD results were evaluated qualitatively using the software package *DiffraC Plus* (Bruker-AXS) combined with the PDF (powder diffraction file) database. For the quantitative Rietveld refinement, the program *BGMN* was used (Bergmann *et al.*, 1998), which includes a fundamental-parameter approach to model the peak profiles (Cheary and Coelho, 1992). To predetermine the instrument-dependent part of the diffraction profile, a ray-tracing procedure was performed. The structural data for the minerals were taken from the ICSD (Inorganic Crystal Structure Database, FIZ, Karlsruhe, Germany) with minor changes. For all minerals (except halloysite) only lattice parameters, peak-broadening parameters, and (if necessary) corrections for preferred orientation were refined with physically reasonable constraints. As non-structural parameters, the zero point, the sample-displacement error, and a Lagrange polynomial of 9<sup>th</sup> degree for background modeling (samples 10–16) were refined. Due to its X-ray amorphous nature, allophane produces a strong modulated diffraction line, which, to date, has not been simulated by Rietveld-compatible intensity calculations. *BGMN* offers the option to describe a background line by an additional user-defined measurement file. This measured data is scaled linearly during the refinement. The feature was used to describe the contribution of the

allophane content in samples 1 to 9. For that, a highly enriched allophane sample was measured (<0.2  $\mu\text{m}$  fraction). The sharp peaks from the quartz impurity in the sample were subtracted and the line was smoothed. By this procedure, in combination with the known content of the internal standard, fitting the powder pattern was possible and the allophane content was quantified indirectly.

Samples 10–16 contain halloysite, consisting of tubular, rolled, partly hydrated, kaolinite-like layers. This degree of disordering prevented the application of traditional structure-describing methods. Because the effect of enrolling layers produces a powder pattern which is similar to that of a turbostratically disordered layer structure, a super-cell approach was used to approximate the halloysite structure. This method has been used successfully to describe smectite powder patterns within the Rietveld refinement (Ufer *et al.*, 2004) and regards the diffraction effect of the disordered layer structure as diffraction from only one layer, ignoring any possible type of ordering. In the case of halloysite, this structural model is an oversimplification, but for the purpose of quantification it provides reasonable values. Due to an unbalanced hydration state, most halloysites show a non-rational series of 001 peaks. Thus far, Rietveld refinement has been unable to handle this kind of disorder. To overcome this drawback in the present study, the refinement of the halloysite-containing samples started at  $14^\circ 2\theta$  and the 001 reflection at  $12^\circ 2\theta$  ( $d = 7.4 \text{ \AA}$ ) was omitted. The 002 reflection at  $24.5^\circ 2\theta$  ( $d = 3.6 \text{ \AA}$ ) was the only basal (00 $l$ ) reflection with a considerable intensity contribution. By choosing a lattice constant,  $c$ , which is suitable to fit the 002 reflection, the whole powder pattern can be refined. The error caused by this uncertainty is relatively small as most of the intensity of the powder pattern stems from non-basal reflections.

#### Summary of XRD-Rietveld method

- McCrone mill using agate grinding elements and an internal standard (10.0 wt.% zincite or corundum);
- Record powder XRD pattern on a diffractometer which can be described geometrically by a fundamental-parameter approach to model the peak profiles (Cheary and Coelho, 1992);
- Indirect, preferential determination (Walenta and Füllmann, 2004) of the amount of X-ray amorphous compounds using *Autoquan*® or *BGMN* by recalculating the corundum/zincite content to 10.0 wt.%.

#### Mössbauer spectroscopy

Mössbauer spectra were obtained on the samples, as received, at liquid He temperature (nominally 4.2 K) and room temperature (nominally 298 K). The instrument was a custom-built device from Web Research, Inc. (Edina, Minnesota, USA) consisting of a constant-acceleration drive system operating in the triangular waveform mode

in conjunction with a Janis Model SHI-850-5 closed-cycle cryostat capable of cooling the sample from ambient temperature to liquid He temperature. The gamma-ray source was  $^{57}\text{Co}$  dispersed as 10% in a thin Rh foil and spectra were calibrated relative to a 7  $\mu\text{m}$  thick foil of  $\alpha\text{-Fe}$ . Mössbauer hyperfine parameters, *i.e.* isomer shift ( $\delta$ ), quadrupole splitting ( $\Delta$ ), and magnetic hyperfine field ( $B_{\text{hf}}$ ), were calculated by a least-squares fitting program, assuming Lorentzian line shapes. These parameters generally reflect the oxidation state, symmetry of the surrounding electrostatic field, and extent of magnetic exchange interaction among the Fe ions in the clay, respectively. The relative peak areas were used to estimate the relative abundance of each phase. This method lacks reliability as a quantitative method, however, because the recoil-free fractions of the Fe in the various phases and oxidation states are unknown (comparing areas assumes they are all equal) and the detection limit and resolution are on the order of  $\pm 5\%$ .

## RESULTS AND DISCUSSION

#### Extraction methods

Results from the various extraction methods (Table 1) revealed that the  $\text{Al}_p$  (pyrophosphate extraction) content was small, indicating that little Al is present in the organic complexes. The value of  $\text{Al}_d$  (dithionite extraction) is commonly believed to represent the amount of Al substituted in Fe (oxyhydr)oxides, but in the present samples it also correlates (although weakly) with the allophane content. The dithionite solution may have dissolved some Al from allophane. A hypothetical alternative explanation for the correlation between  $\text{Al}_d$  and allophane is that Fe could be finely dispersed in the allophane structure. When attacked by dithionite, some of this Fe could be partially dissolved, thus weakening the allophane structure and releasing some of the Al also. The  $\text{Fe}_d$  values theoretically represent the total amount of Fe (oxyhydr)oxides.

According to Buurmann *et al.* (2001) and Dohrmann *et al.* (2002), the accuracy of the allophane contents determined by these standard extraction methods (Table 1) is questionable. Both of these studies proved the incomplete dissolution of allophane, probably caused by the large allophane content. To overcome this problem, the solid:liquid ratio was varied rather than repeating the extraction steps. The disadvantage of carrying out multiple extractions is a degradation of accuracy because the solid-liquid separation procedure could either leave some dissolved Al in the solid or could lose Al during washing steps. This approach robustly improves the dissolution of partially soluble phases. The reaction time was also increased from 4 to 48 h and the temperature was increased from 25 to 60°C.

Results from this approach (Figure 1) clearly demonstrated that altering the reaction time, temperature, and solid:solution ratio alters the result obtained

Table 1. Ammonium oxalate (o), dithionite (d), and pyrophosphate (p) extraction and calculation of allophane content according to Parfitt and Wilson (1985). Al/Si ratio = 1.35 (Kaufhold *et al.*, 2009).

Sample	Fe <sub>o</sub> (g/kg)	Si <sub>o</sub> (g/kg)	Al <sub>o</sub> (g/kg)	Fe <sub>d</sub> (g/kg)	Si <sub>d</sub> (g/kg)	Al <sub>d</sub> (g/kg)	Fe <sub>p</sub> (g/kg)	Si <sub>p</sub> (g/kg)	Al <sub>p</sub> (g/kg)	Allophane (wt.%)
PM4-1	14	57	84	22	8	18	0.5	2	3	32
PM4-2	14	72	104	31	9	22	0.3	1	3	40
PM4-3	12	67	99	39	8	21	0.2	1	3	37
PM4-4	10	64	97	25	8	17	0.1	1	3	36
PM4-5	13	81	119	50	9	25	0.3	1	3	45
PM4-6	15	87	126	61	13	32	0.2	1	4	48
PM4-7	6	69	110	33	11	24	0.1	1	4	39
PM4-8	8	48	75	82	24	46	0.4	1	3	27
PM4-9	7	44	66	81	17	37	0.4	1	3	25
PM4-10	4	17	26	23	5	9	1.1	2	3	9
PM4-11	7	17	27	38	9	16	1.0	2	3	10
PM4-12	1	1	2	44	3	7	1.4	2	2	1
PM4-13	2	1	2	183	8	19	0.3	1	0	1
PM4-14	1	1	2	174	10	19	0.1	1	1	1
PM4-15	0	0	1	30	1	3	0.1	2	2	0
PM4-16	0	1	1	52	2	4	0.1	1	1	0

and further indicated that the allophane content of sample PM4-6 could be as large as 60–75 wt.% instead of <50 wt.% as obtained by the standard extraction method. (The observed scatter or variability in the data reported in Figure 1 is probably due to the small sample mass used to obtain the small solid:liquid ratios.) These results fail to clarify, however, whether Al and Si were dissolved from other minerals (feldspar, halloysite, *etc.*). Based on these observations, a solid:liquid ratio of 2 to 4 (48 h extraction at 60°C) was considered to be a more realistic reflection of the allophane content of the materials studied. These conditions, *i.e.* solid:liquid ratio of 1 g/L, 48 h extraction time, and 60°C, were, therefore, adopted for all samples, and the values obtained were labeled ‘modified extraction.’ Both the

conventional and modified extraction results were compared with XRD results.

#### XRD results and Fe-mineral identification

Quantitative results obtained by XRD (Table 2) were derived from Rietveld refinement without taking any chemical information into account; due to the existence of different phases with varying and unknown degrees of disorder (*e.g.* halloysite), however, validation of these XRD results by chemical analysis was deemed necessary. This was accomplished by summing the chemical elements of all minerals according to their content and then comparing the sums with the measured chemical composition. The accuracy of this method depends heavily on the quality of the chemical data, particularly

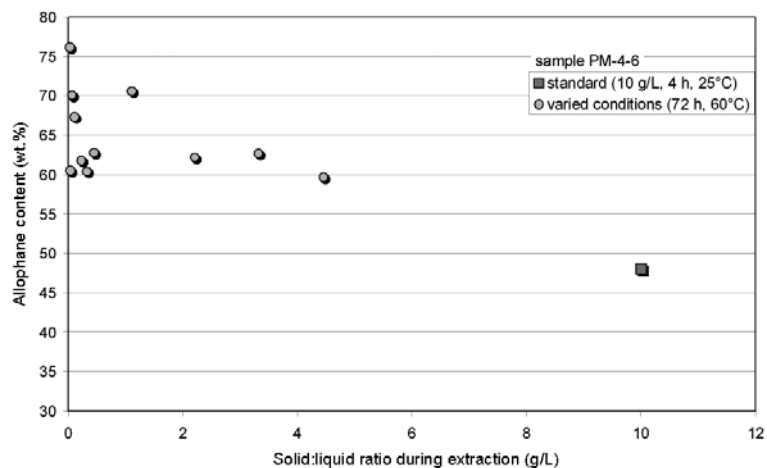


Figure 1. Effect of variation of the solid:liquid ratio, temperature, and reaction time on the amount of allophane detected (sample PM4-6; Kaufhold *et al.*, 2009).

Table 2. Quantitative mineralogical composition of the allophane samples as calculated by the Rietveld program *BGMN* ("0" = 0.1–0.4 wt.%).

Sample PM Depths (m)	Allophane facies									Halloysite facies						
	4-1 0.5	4-2 1.5	4-3 2	4-4 3	4-5 4	4-6 5	4-7 6	4-8 7	4-9 8	4-10 9	4-11 10	4-12 11	4-13 12	4-14 13	4-15 14	4-16 14.5
X-ray amorphous (allophane, ± imogolite (?) ± Fe oxides (?) )	53	69	64	68	74	78	73	55	54	29	36	8	9	9	7	7
Halloysite								14	24	47	43	77	59	54	81	77
Gibbsite	1							8	2	5	2	1				
Quartz	5	6	6	2	3	2	5	3	2	3	4	5	4	4	5	4
Cristobalite	4	3	4	4	2	3	3	3	3	3	3	2	1	1	1	2
Hornblende	10	7	7	3	7	6	9	4	4	5	6					
Feldspar	20	10	11	16	6	2	5									
Goethite	2	4	5	1	6	7	4	12	11	7	4	6	25	31	5	8
Magnetite	3	2	2	4	2	0	0	0	0	1	2					
Dolomite	1	0	0	1	0		0									
Ilmenite	1	0	1	1	0	1	0	1	1	1	1	1	2	1	1	1
Anatase									0	0	0	1	0	1	1	1

of the main components. In this study, that component was allophane (X-ray amorphous), for which the Al:Si ratio was known and posed no problem. Iron, on the other hand, was a significant problem.

Kaufhold *et al.* (2009) found rather different Fe contents within the cloud-like allophane aggregates. No general structural formula of the allophane can, therefore, be given unless the distribution of Fe is clarified. Accordingly, XRF, XRD, and extraction values were compared. This required some approximations (*e.g.* Fe<sub>2</sub>O<sub>3</sub> content of goethite = 90 wt.%) in order to be able to compare the values derived from the different methods (all converted to Fe<sub>2</sub>O<sub>3</sub> in wt.%). The resulting

error was small, indicating that the procedure described below is suitable for the investigation of Fe mineral distribution (Table 3).

In order to make valid comparisons with XRF elemental analysis, the dithionite extraction data (obtained as g/kg based on material dried at 105°C) were converted to wt.% oxide. The difference between XRF and dithionite values ('Diff<sub>Fe<sub>2</sub>O<sub>3</sub></sub>' in Table 3) was then calculated and, in the case of allophane (4-1 to 4-9), could represent Fe minerals such as magnetite, which are incompletely dissolved by the dithionite extraction method. In the case of halloysite facies (4-10 to 4-16), however, the magnetite content was too small to account

Table 3. Comparison of XRF, XRD, and extraction data on the basis of Fe<sub>2</sub>O<sub>3</sub> contents.

	Fe <sub>2</sub> O <sub>3</sub> XRF (wt.%)	Fe dithionite (g/kg)	Fe <sub>2</sub> O <sub>3</sub> dithionite (wt.%)	Diff <sub>Fe<sub>2</sub>O<sub>3</sub></sub> XRF-dith. (wt.%)	Magnetite XRD <sub>quan</sub> (wt.%)	Fe oxalate (g/kg)	Fe <sub>2</sub> O <sub>3</sub> oxalate (wt.%)	Goethite XRD <sub>quan</sub> (wt.%)	Fe <sub>2</sub> O <sub>3</sub> (goethite) XRD <sub>quan</sub> (wt.%)
PM4-1	8	22	3	5	3	14	2	2	2
PM4-2	7	31	4	3	2	14	2	4	3
PM4-3	9	39	6	3	2	12	2	5	5
PM4-4	10	25	4	6	4	10	1	1	1
PM4-5	10	50	7	3	2	13	2	6	6
PM4-6	10	61	9	1	0	15	2	7	7
PM4-7	7	33	5	3	0	6	1	4	4
PM4-8	12	82	12	0	0	8	1	12	10
PM4-9	12	81	12	0	0	7	1	11	10
PM4-10	11	23	3	7	1	4	1	7	6
PM4-11	11	38	5	6	2	7	1	4	4
PM4-12	8	44	6	2		1	0	6	5
PM4-13	26	183	26	0		2	0	25	22
PM4-14	26	174	25	1		1	0	31	28
PM4-15	10	30	4	5		0	0	5	4
PM4-16	6	52	7	-2		0	0	8	8

for the XRF-dithionite difference. No difference between XRF and dithionite was found in the goethite rich layer (4-13 + 4-14). In this layer Fe occurs only as goethite. The differences observed for the other samples of the halloysite facies may be explained by Fe incorporated in the halloysite structure. This, however, has yet to be determined.

Oxalate-extractable Fe phases were found in the allophane facies in only small amounts and almost none was found in the halloysite facies. Because of the small amount of oxalate-extractable Fe, a good correlation was found between dithionite-soluble Fe and goethite determined by XRD, which confirms the quality of the XRD data.

The distribution of Fe in other phases was also deduced by comparing XRD, chemical, and selective dissolution results. For example, in sample 4-6 the total Fe<sub>2</sub>O<sub>3</sub> content was 10 wt.%. The weight loss by dithionite extraction was 9 wt.% Fe<sub>2</sub>O<sub>3</sub>. The difference (1 wt.%), within experimental error, can be explained by 0.5 wt.% magnetite and 0.8 wt.% ilmenite (XRD data), which, typically, are partially or mostly insoluble by the dithionite method. A large amount (7 wt.% Fe<sub>2</sub>O<sub>3</sub>) of the dithionite-extractable Fe is attributable to goethite, but the phase containing the remaining 2 wt.% Fe<sub>2</sub>O<sub>3</sub> has yet to be identified. It could be ferrihydrite, another Fe mineral exhibiting similar short range order, or in the structure of the allophane.

In this context, note that ferrihydrite cannot be differentiated from allophane by XRD due to their both having short-range order. Accordingly, the allophane

(+imogolite) content was obtained by subtracting the oxalate-soluble Fe from the total amount of X-ray-amorphous phases. However, this correction is valid only if the oxalate-soluble Fe occurs in phases that are separate from the allophane. Conceivably, the oxalate-soluble Fe could occur in the primary allophane particle. According to Kaufold *et al.* (2009), Fe was found within the cloud-like allophane aggregates ( $\varnothing$  0.5–1  $\mu$ m) in varying amounts. No specific Fe minerals could be identified. Hence, varying amounts of Fe were assumed to be dispersed in the allophane structure or on its surfaces. The XRD investigation of the <0.2  $\mu$ m fraction in the present study proved the existence of goethite. Mössbauer spectroscopy (Figure 2) confirmed this finding, as indicated by the hyperfine parameters of the magnetically ordered spectra at LHe temperature (Table 4). Goethite clearly dominated the Fe phases in the sample, even though some hematite and silicate structural Fe(III) and Fe(II) were observed. The identity of the 2 wt.% oxalate-soluble Fe could not be discerned by these methods, however.

Chemical analysis of two allophane samples (PM4-6 and PM4-10) revealed a total Fe content of 6.5 (9.3 Fe<sub>2</sub>O<sub>3</sub>) and 6.0 (8.6 Fe<sub>2</sub>O<sub>3</sub>) wt.%, respectively, of which 9.1% and 8.1% of the Fe was present as Fe(II), respectively. The Mössbauer spectra of these same samples, obtained at room (RT) and liquid He (LHe) temperatures (Figure 2, Table 4), revealed that at least 92% and 97%, respectively, of the Fe was present in an Fe (oxyhydr)oxide form.

Table 4. Mössbauer hyperfine parameters of samples PM4-6 and PM4-10 at 298 K (RT) and 4.2 K (LHe).

Sample	<i>T</i> (K)	Fe phase	$\delta$ (mm/s)*	$\Delta$ (mm/s)*	$\Gamma$ (mm/s)*	<i>B</i> <sub>hf</sub> (T)	RA (%)*
PM4-6	RT	Fe(III)	0.355(5)	0.51(1)	0.353(5)	–	42(2)
			0.356(2)	0.84(1)	0.41(1)	–	33(3)
		Fe(II)	1.15(1)	2.40(3)	0.57(3)	–	7.3(2)
		Hematite	0.360(9)	–0.17(1)	0.9(3)	49.35(6)	17.6(6)
PM4-6	LHe	Hematite	0.49(4)	–0.18(1)	0.71(2)	51.05(8)	30(2)
			0.48(2)	–0.23(4)	0.49(2)	48.84(3)	26(2)
		Goethite	0.48(1)	–0.17(1)	0.56(3)	46.6(1)	17(2)
		Fe(III)	0.48(4)	0.97(6)	1.5(2)	–	8(1)
		Allophane	0.50(1)	–0.15(2)	0.9(3)	43.0	19(1)
PM4-10	RT	Fe(III)	0.350(1)	0.506(6)	0.338(6)	–	55(3)
			0.348(2)	0.84(2)	0.37(1)	–	26(3)
		Fe(II)	1.20(3)	2.27(6)	0.74(6)	–	7.0(5)
		Hematite	0.32(4)	–0.17(4)	1.6(1)	48.8(2)	12(1)
PM4-10	LHe	Goethite	0.49(1)	–0.28 (8)	0.56(2)	48.14(6)	37(1)
			0.46(1)	–0.1 <sup>†</sup>	0.94(5)	45.8(2)	16(1)
		Hematite	0.47(2)	–0.21(4)	0.55(1)	49.61(4)	44(1)
		Fe(III)	0.23(4)	0.60(4)	0.8(1)	–	3(1)

<sup>†</sup> Held constant during the fitting

\* Value in ( ) represents error in last digit

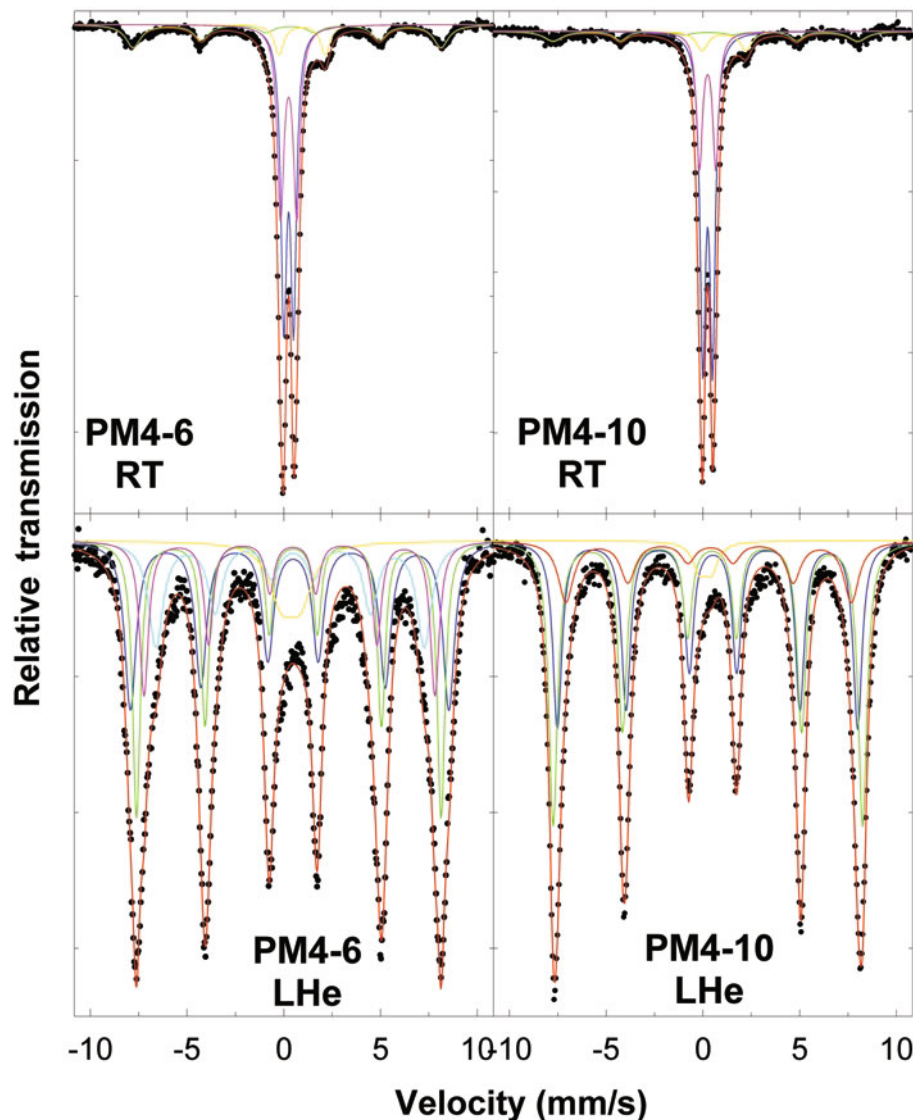


Figure 2. Mössbauer spectra of samples PM4-6 and PM4-10 at 298 K (RT) and 4.2 K (LHe). See Table 4 for hyperfine parameters.

For sample PM4-6, the observed sextet in the Mössbauer spectrum at LHe temperature was asymmetrically broadened toward the inside or lower absolute velocity side of the peaks, leading to a fit requiring a minimum of four over-lapping component sextets with magnetic hyperfine fields ( $B_{hf}$ ) of 51, 48.8, 46.6, and 43 T (Table 4). These values are consistent with the presence of some poorly ordered hematite but with the Fe phases being dominated by goethite.

Treatment of this sample with acid ammonium oxalate or citrate-bicarbonate-dithionite (CBD) at 70°C removed all of the Fe from the sample except residual amounts of 7.9 wt.% and 2.7 wt.%, respectively. The residual Fe in the CBD-treated sample was identified by Mössbauer spectroscopy as being distributed about equally between a poorly crystalline hematite and a

structural silicate phase. The small difference in Fe removed by these two methods indicates that the Fe phases must be rather poorly crystallized. Evidence from the Mössbauer study does not contradict this finding. The room-temperature spectrum contains a broadened sextet, attributed to poorly ordered hematite, comprising <20% of the total Fe.

The analysis of sample PM4-10 led to a similar conclusion, except the Fe phases seemed to be somewhat less complex. The Mössbauer spectrum at LHe temperature consisted of an overall sextet pattern with individual peaks being less broadened than in the case of sample PM4-6. The Fe was assigned to phases consistent with poorly ordered hematite, goethite, and a silicate structural environment. The sextet due to hematite in the RT spectrum was very broad and accounted for only 12% of

the Fe. Because the difference in relative area of the sextet for hematite between the RT and LHe spectra is so large (12% compared to 44%), even larger than in the case of sample PM4-6, the hematite is clearly not well crystallized. The  $B_{hf}$  value of 49.6 T for this sample is also very small for hematite, suggesting that this phase is poorly crystalline. The similar levels of Fe dissolution found by the oxalate and CBD treatments of this sample, *i.e.* 0.3 wt.% and 0.1 wt.% residual Fe, respectively, confirmed this finding and extended it to all of the Fe (oxyhydr)oxides in the sample. Oxidation-state analysis and Mössbauer spectra obtained after CBD treatment revealed similar results to those of sample PM4-6.

#### Comparison of XRD and extraction methods for allophane content

The allophane contents determined by standard extraction techniques were smaller than those determined by XRD Rietveld refinement (black circles in Figure 3). Modification of the extraction conditions – as deduced from Figure 1 – obviously led, however, to the dissolution of halloysite (squares in Figure 3, changes marked by arrows) as indicated by significantly more being dissolved compared to both the standard extraction and XRD methods. In conclusion, the modification of the extraction conditions led to reasonable results if halloysite was absent (allophane-rich samples of allophane facies).

#### Water content

Allophane, like smectite, is able to adsorb appreciable amounts of water from the atmosphere. Hence, the water content of such minerals varies depending on the ambient conditions. In the case of allophane and

smectite, this water is part of the mineral and influences the bulk density. Smectites swell in water, which generally decreases the smectite bulk density and affects the crystal structure by increasing the  $d$  spacing and by incorporating additional water molecules. In contrast, allophane bulk densities increase because most of the adsorbed water reaches the inner part of the hollow sphere, which adds mass without changing the volume. Accordingly, water adsorption increases the density of the particle, which, of course, also affects the (gravimetric) allophane content within a mixture. The maximum water-adsorption capacity of allophane depends heavily on sample pre-treatment, so specifying a general value is not possible. Allophane can undoubtedly adsorb as much as 20 wt.% water at 50% r.h. (referred to sample mass dried at 105°C), however. This means that the allophane content of a soil containing 50 wt.% allophane at 105°C increases to 60 wt.% if the same sample is stored at 50% r.h. In conclusion, for the accurate determination of the allophane content, a reference state (*e.g.* dried at 105°C) must be provided; 105°C is generally accepted in clay science. Allophane is, however, known to hold appreciable amounts of adsorbed water even at 105°C (see the DTA curves for allophane sample PM4-7 and the water content determined after 24 and 72 h; Figure 4), so the suitability of this reference state is questionable.

Differential thermal analysis (Figure 4) revealed that the dehydration maximum was at  $\sim 150^\circ\text{C}$ . Considering the position of the dehydration peak, 250°C appears to be a more suitable reference temperature where all water is removed. Of course, dehydration not only depends on temperature but also on time and r.h. Upon drying at 60°C for 24 h, the allophane lost 11 wt.% of water (no changes

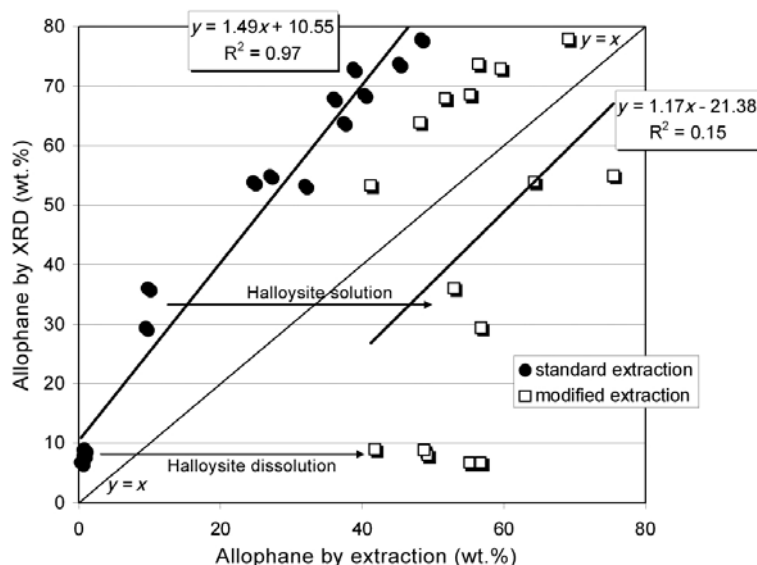


Figure 3. Comparison of extraction data and XRD Rietveld analysis for the quantification of allophane.



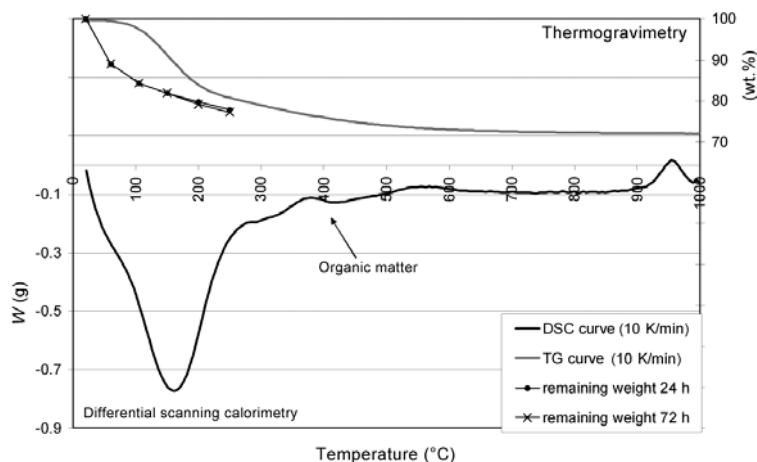


Figure 4. DTA of allophane sample PM4-7 (sample equilibrated at 50% r.h. prior to analysis; heating rate 3 K/min) and water content determined after 24 and 72 h, respectively.

after 72 h; sample weight 1 g, double specimen). After storage at 105°C, the allophane lost 16 wt.% of its water, the equilibrium again was attained after 24 h. Increasing the temperature to 150°C, 200°C, and 250°C yielded additional 2 wt.% increments of water loss with each of these temperature intervals (18, 20, and 22 wt.% in total). In the cases of 200°C and 250°C, 72 h drying was required in order to reach equilibrium conditions.

The water content determined at 105°C probably does not represent a specific type of water (*e.g.* '1-layer-water') and some water molecules adsorbed to the inner part of the hollow spheres should still be present. From this point of view the reference temperature of 105°C is considered to be imperfect, but DTA results (Figure 4) fail to suggest a reasonable alternative. Note also that the allophane quickly 'readsorbs' the 2 wt.% water which is

lost between 105 and 150°C, which in turn affects analytical accuracy. In conclusion, 105°C was considered to be the optimum reference temperature.

As stated above, dried allophane is known to quickly readsorb water from the atmosphere (or even desorb water, depending on the ambient conditions). Whether this water adsorption affects the XRD results and whether ambient conditions need to be controlled during measurement are still open to question. One allophane sample (PM4-7) was, therefore, measured at different r.h. (Figure 5). The results clearly indicated that the r.h., and hence the water content of the allophane, had no effect on the XRD results; in other words, XRD is insensitive to different allophane densities (caused by different water contents) which stresses the importance of referring allophane contents to a reference dry state.

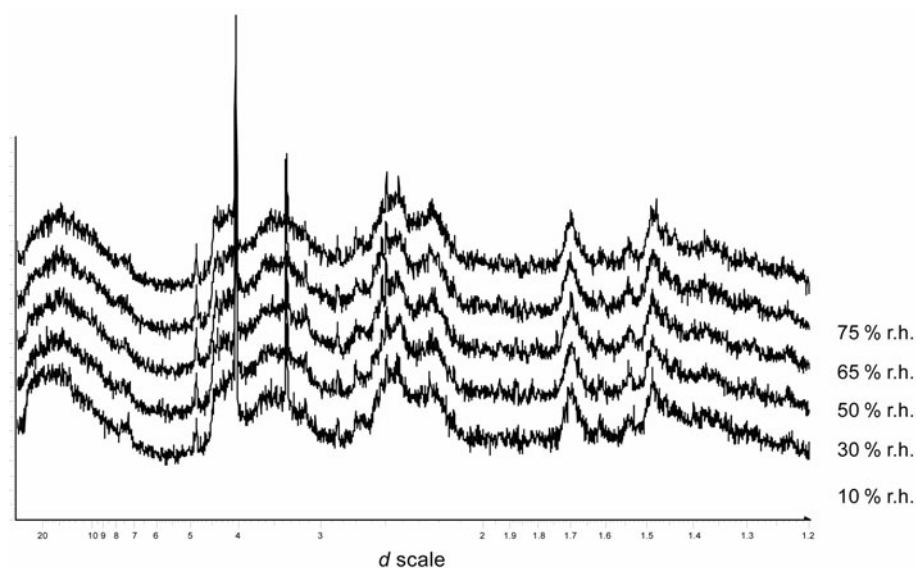


Figure 5. XRD patterns of allophane sample PM4-7 measured at different relative humidities (r.h.).

## SUMMARY AND CONCLUSIONS

The standard extraction technique (ammonium oxalate) for the quantification of allophane systematically underestimates the allophane content, which is particularly true in the case of soils with large allophane contents. The modification of extraction conditions may lead to the additional dissolution of halloysite. On the other hand, the XRD Rietveld technique can provide reasonable results. Special care is required, however, with respect to the selection of appropriate structural models.

Concerning the Fe minerals, consistent quantitative results were obtained by the Rietveld XRD technique and the common extraction methods. Hence, Fe-extraction methods are still considered valuable tools for the complex quantification of clays and soils (in contrast to the allophane extraction methods).

The allophane of the profile investigated in the present study apparently contains very fine-grained goethite being dispersed in the cloud-like allophane aggregates. Although probably closely attached to the allophane, goethite had to be quantified as a separate phase and Fe substitution in the allophane lattice was found to be small.

Allophane is known to adsorb appreciable amounts of water depending on the ambient conditions. Accordingly, the weight of this mineral within the sample changes. Therefore, 105°C is commonly used as the reference temperature. From DTA, no preferable alternative temperature was identified. Different water contents do not affect the XRD intensities. Hence, no special control of the r.h. throughout XRD measurements is required.

## REFERENCES

- Bergmann, J., Friedel, P., and Kleeberg, R. (1998) BGMN – a new fundamental parameters based Rietveld program for laboratory X-ray sources, its use in quantitative analysis and structure investigations. Commission of Powder Diffraction. *International Union of Crystallography, CPD Newsletter*, **20**, 5–8.
- Blakemore, L.C., Searle, P.L., and Daly, B.K. (1981) *Methods for Chemical Analysis of Soils*. Scientific Report 10A, New Zealand Soil Bureau, Department of Scientific and Industrial Research, Lower Hutt, New Zealand.
- Blakemore, L.C., Searle, P.L., and Daly, B.K. (1987) *Methods for Chemical Analysis of Soils*. Scientific report No. 80. New Zealand Soil Bureau, Department of Scientific and Industrial Research, Lower Hutt, New Zealand.
- Buurman, P., Nakken, N., Meijer, E.L., and Garcia-Rodeja, E. (2001) Repeated oxalate extraction of European allophanic soils. P. 63 in: *Volcanic Soils: Properties, Processes and Land Use*. Porta Delgada, S. Miguel, Azores, Portugal.
- Cheary, R.W. and Coelho, A.A. (1992) A fundamental parameters approach to X-ray line-profile fitting. *Journal of Applied Crystallography*, **25**, 109–121.
- Dahlgren, R.A. (1994) Quantification of allophane and imogolite. Pp. 431–451 in: *Quantitative Methods in Soil Mineralogy* (R.J. Luxmoore, editor). Soil Science Society of America, Madison, Wisconsin, USA.
- Dohrmann, R., Meyer, I., Kaufhold, S., Jahn, R., Kleber, M., and Kasbohm, J. (2002) Rietveld based-quantification of allophane. *Mainzer Naturwissenschaftliches Archiv*, **40**, 28–30.
- Harsh, J. (2000) Poorly crystalline aluminosilicate clays. Pp. F169–F182 in: *Handbook of Soil Science* (M.E. Sumner, editor). CRC Press, Boca Raton, Florida, USA.
- Kaufhold, S. (2007) Ecuadorian Allophane. *Industrial Minerals*, May 2007, p. 95.
- Kaufhold, S., Kaufhold, A., Jahn, R., Brito, S., Dohrmann, R., Hoffmann, R., Gliemann, H., Weidler, P., and Frechen, M. (2009) A new massive deposit of allophane raw material in Ecuador. *Clays and Clay Minerals*, **57**, 72–81.
- Parfitt, R.L. (1990) Allophane in New Zealand – a review. *Australian Journal of Soil Research*, **28**, 343–360.
- Parfitt, R.L. (2009) Allophane and imogolite: role in soil biogeochemical processes. *Clay Minerals*, **44**, 135–155.
- Parfitt, R.L. and Wilson, A.D. (1985) Estimation of allophane and halloysite in three sequences of volcanic soils, New Zealand. Pp. 1–8 in: *Volcanic Soils, Vol. 7* (E. Fernandes and D.H. Yaalon, editors). Catena Verlag, Reiskirchen, Germany.
- Schwertmann, U. (1964) Differenzierung der Eisenoxide des Bodens durch Extraktion mit Ammoniumoxalat-Lösung. *Zeitschrift für Pflanzenernährung Düngung und Bodenkunde*, **105**, 194–202.
- Ufer, K., Roth, G., Kleeberg, R., Stanjek, H., Dohrmann, R., and Bergmann, J. (2004) Description of X-ray powder pattern of turbostratically disordered layer structures with a Rietveld compatible approach. *Zeitschrift für Kristallographie*, **219**, 519–527.
- Ufer, K., Stanjek, H., Roth, G., Dohrmann, R., Kleeberg, R., and Kaufhold, S. (2008) Quantitative phase analysis of bentonites by the Rietveld method. *Clays and Clay Minerals*, **56**, 272–282.
- Walenta, G. and Füllmann, T. (2004) Advances in quantitative XRD analysis for clinker, cements, and cementitious additions. *Powder Diffraction*, **19**, 40–44.

(Received 12 May 2009; revised 15 June 2010; Ms. 319; A.E. W.P. Gates)